X-ray telescope deformation reduction using stress relief features

Anjelica Molnar-Fenton[a], Alexander R. Bruccoleri[a], Youwei Yao[b],
Ralf K. Heilmann[b], Mark L. Schattenburg[b]
[a]Izentis LLC, PO Box 397002, Cambridge, MA, USA 02139-7002
[b]Space Nanotechnology Lab, MIT, 70 Vassar St., Cambridge, MA, USA 02139

ABSTRACT

A stress relief technique is presented to reduce the distortion of X-ray optics from adhesive shrinkage at bonding points. The bonding distortions are particularly relevant for thin-shell mirror optics and need to be minimized to meet sub-arcsecond angular resolution goals. Thin-shell optics are critical to achieving large collecting areas for X-ray telescopes, such as the Lynx mission concept. A localized topography modification of the optic surrounding the adhesive point has been explored to reduce global distortion. Previous efforts utilized finite element analysis (FEA) to study removal of material around the adhesive joint in an annulus pattern, creating a trench. Current work has improved the finite element model for the trench design as well as shown an experimental verification. These experiments involve using silicon wafers as test mirrors and silicon oxide to mimic stress induced by adhesive shrinkage. The silicon oxide is encompassed by the trench etch, which is used to demonstrate a reduction in global deformation. We present the recent progress made with this stress relief technique.

Keywords: x-ray, Lynx, telescope, optics, stress relief

1. INTRODUCTION

1.1 Stress Localization Concept Overview

In this paper, we present an approach to reduce distortion of mirror surfaces in thin-shell X-ray telescopes due to epoxy shrinkage at the bonding points[1]. The premise behind using segmented optics for X-ray telescope construction has already been shown by the NuSTAR X-ray telescope[2]. The NuSTAR X-ray telescope was built by attaching thin slumped-glass sheets in a stack, using graphite spacers to attach the mirrors together. By stacking mirrors NuSTAR achieved a large effective area[3], although the angular resolution was low, approximately 50 arcseconds half power diameter (HPD)[4]. Currently, the X-ray astronomy optics community is working towards the next flagship X-ray telescope, Lynx X-ray telescope mission concept. Lynx has a width greater than two square meter effective collecting area and angular resolution of 0.5 arcseconds HPD[5].

In order to meet the goals of large collecting area and high angular resolution, different approaches have been considered for developing the telescope's optics. The meta-shell concept is one particular approach, which is described in McClelland et al.[6] and has been selected for the Lynx Design Reference Mission. The meta-shell concept works by nesting thin monocrystalline silicon mirrors around a support shell. Each mirror optic rests on four posts that are lapped and polished to a precise height. Once the desired height is achieved, posts and mirror are epoxied together. This process continues until there is a stack of thin mirrors tens of layers deep. The final design consists of multiple shells assembled and aligned together to produce the entire X-ray telescope optic.

To address mirror distortion due to bonding, a stress relief technique for thin X-ray optics is presented. When epoxy is used to mount mirrors to posts, the epoxy introduces a compressive stress on the surface of the optic. From the epoxy stress a tensile reaction on the mirror backside creates bending and distortion. This stress degrades telescope resolution by causing deformation over the entire mirror surface. A local topography change is proposed to reduce distortion from bonding stress. The proposed idea is to etch a trench around the stress point on the optic. The trench will surround the epoxy bond area, and mostly limit the deformation to the area encircled by the trench.

Optics for EUV, X-Ray, and Gamma-Ray Astronomy IX, edited by Stephen L. O'Dell, Giovanni Pareschi, Proc. of SPIE
Vol. 11119, 111191T · © 2019 SPIE · CCC code: 0277-786X/19/$21 · doi: 10.1117/12.2530572

Downloaded From: https://www.spiedigitallibrary.org/conference-proceedings-of-spie on 11 Sep 2019
Terms of Use: https://www.spiedigitallibrary.org/terms-of-use

2. METHODOLOGY

2.1 Design and Fabrication Process

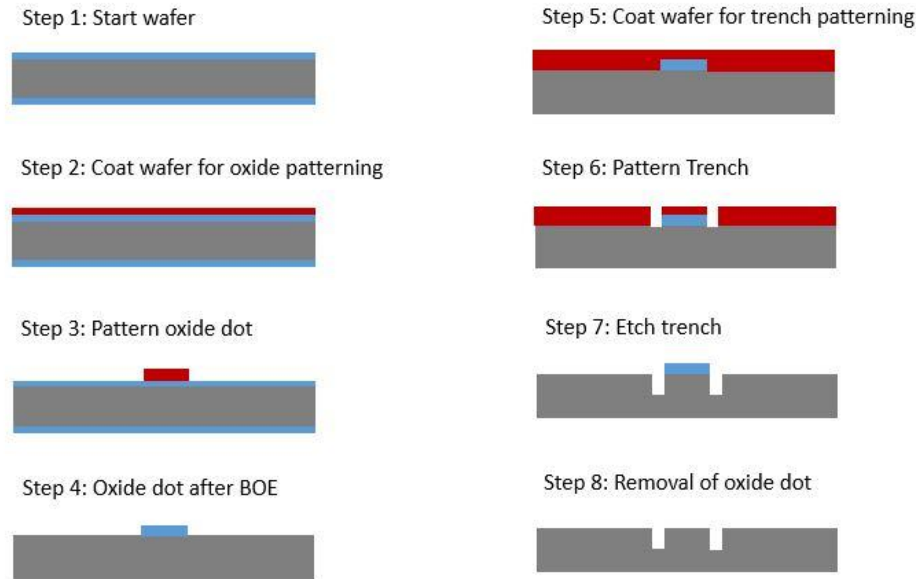

Figure 1. Process flow chart of the steps to create an oxide dot on a silicon wafer with a trench etched around it.

A design and fabrication process was created to evaluate the trench etch as a stress relief concept (Figure 1). For this demonstration an oxide dot was used instead of an epoxy dot since it is a simple way to produce small regions of repeatable compressive stress. To create this design a 500 µm-thick silicon wafer with 2 µm of thermal oxide grown on both sides was used, as shown in Step 1. Then a roughly 12 µm-thick layer of photoresist was coated on the top (Step 2). Next, a 4 mm-diameter oxide dot was lithographically patterned into the photoresist and developed, leaving a 4 mm photoresist dot in the center as shown in Step 3. The wafer from Step 3 was etched with buffered oxide etch (BOE) until all the unprotected areas were etched away (Step 4). In Step 5, a roughly 12 µm- thick coating of photoresist was added to the wafer shown in Step 4. An annulus was then patterned on the wafer, which, after developing, created a 50 µm-wide ring in the photoresist (Step 6). From there the wafer was etched in a deep reactive ion etch (DRIE) tool. The wafer after DRIE etching is shown in Step 7. The depth shown in Step 7 was determined by the length of the etch process.

2.2 Measurement Process

In an ideal situation, measurements taken at three different steps during the process would be required to fully characterize the stress due to the oxide dot. These measurements would also demonstrate how much reduction was seen when the trench was etched around the dot, if any. The first measurement taken was with a bare wafer with oxide on both sides (Step 1), which was meant to characterize the initial shape of the wafer. The next measurement was performed after the oxide dot was patterned (Step 4) and it measured the deformation of the bare wafer caused by the process of adding an oxide dot. Finally, a third measurement was taken of the same bare wafer with the oxide dot and the trench etch (Step 7), which showed the reduction in deformation due to an added trench. Unfortunately, due to a change in metrology we could not present any data on the schematic in Step 1 because all wafers used for testing already had an oxide dot patterned on the wafer. Instead we used the schematic shown in Step 8 as our reference wafer, recognizing that there was a trench etch in the wafer. We assumed that the trench etch did not add any additional stress to the wafer. The results of these measurements are shown in the following section.

Downloaded From: https://www.spiedigitallibrary.org/conference-proceedings-of-spie on 11 Sep 2019
Terms of Use: https://www.spiedigitallibrary.org/terms-of-use

3. RESULTS AND DISSCUSION

3.1 Results of Simulated Data

To check the validity of the proposed stress relief concept, a FEA model was simulated using the Abaqus software program. We focused on two designs. The first design was the oxide dot simulated on a bare silicon wafer. This result concluded that a 4 mm diameter, 2 µm oxide dot caused 888 nm P-V deformation to a 100 mm diameter, 500 µm - thick wafer (Figure 2). The second design included an annulus of 50 µm width around the oxide dot with a depth variation between 100-300 µm. The addition of a 300 µm trench, as shown in Figure 3, caused the P-V deformation to be 487 nm. All other data for various trench depths are represented in Table 1.

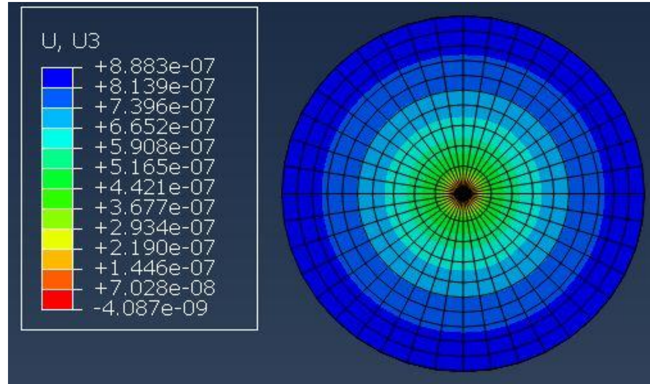

Figure 2. Simulated data shows 888 nm deformation of a silicon wafer with a 4 mm diameter and 2 µm oxide dot with a stress of 300 MPa. The scale bar is in meters.

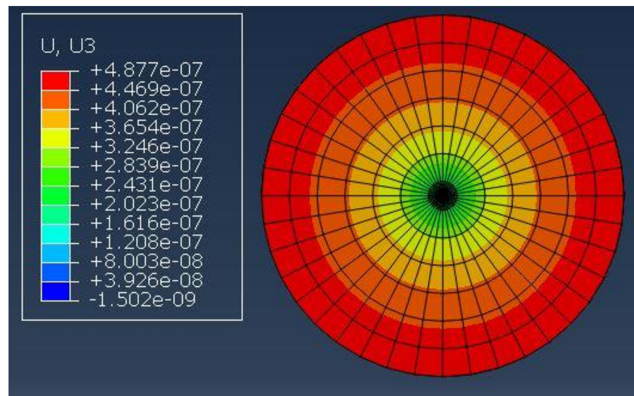

Figure 3. Simulated data shows 487 nm deformation of silicon wafer with the oxide dot and a 300 µm trench etch depth. The oxide dot was 4 mm in diameter and 2 µm thick with a stress of 300 MPa. The scale bar is in meters.

Table 1. Results of simulations of four different wafers designed with different trench depths.

Trench Depth (µm)	P-V Deformation (nm)	P-V deformation reduction (%)
0	888	-
190	718	19.14

Downloaded From: https://www.spiedigitallibrary.org/conference-proceedings-of-spie on 11 Sep 2019
Terms of Use: https://www.spiedigitallibrary.org/terms-of-use

260	648	27.02
300	487	45.15

3.2 Results of Experimental Data

Four wafers went through the proposed trench method outlined in Figure 1. First, the surface height of a wafer with just an oxide dot was measured via an interferometer. The data showed a P-V of 750 nm with an RMS height of 97.17 nm. This was done via a subtraction between the data of a flat bare silicon wafer and a silicon wafer with an oxide dot in the middle (Figure 4). This subtraction analysis process was then repeated for wafers with etch depths of 190 µm, 260 µm and 300 µm. The height maps for the deepest etch (300 µm) is shown in Figure 4 (b) and (c). The key data for the rest of the wafers is outlined in Table 2.

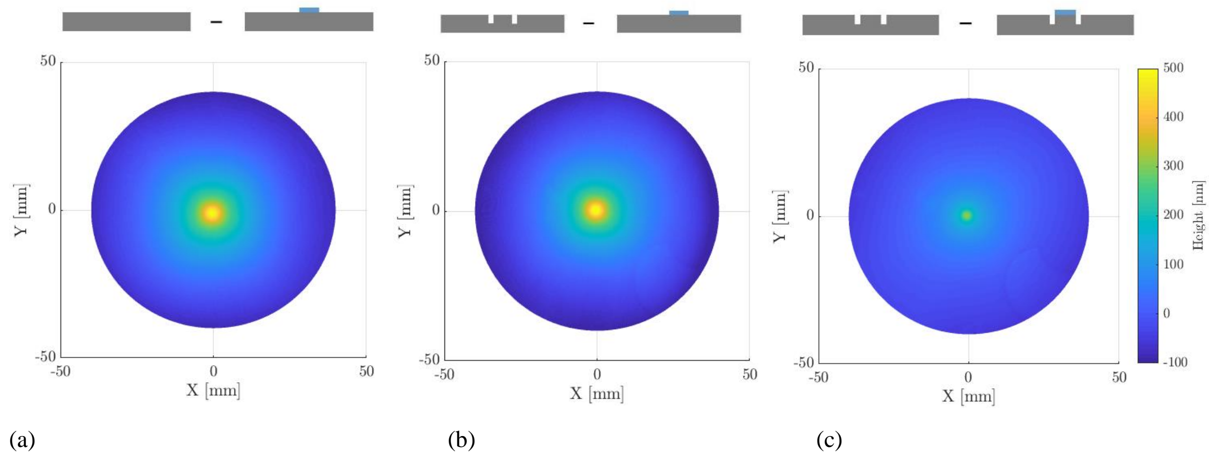

(a) (b) (c)

Figure 4. (a) Top: Schematic illustrating a bare silicon wafer surface height map subtracted from the surface height map of a silicon wafer with oxide dot on it. Bottom: Experimental data of Wafer 1 showing the subtraction performed in the top image. Note that Wafer 1 has no trench etch present in the bare wafer during the subtraction. (b) Top: Schematic illustrating a bare silicon wafer with the trench etch subtracted from a silicon wafer with oxide on it. Bottom: Experimental data of Wafer 4 showing the subtraction performed in the top image. Note that the trench etch into the bare silicon wafer was present for the subtractions done in Wafer 2, 3 and 4. (c) Top: Schematic illustrating a bare silicon wafer with the trench etch subtracted from a silicon wafer with the oxide dot and the trench etch. Bottom: Experimental data of Wafer 4 showing the subtraction performed in the top image. Note that the trench etch into the bare silicon wafer was present for the subtractions done with Wafers 2, 3 and 4.

Table 2. Experimental results of four wafers processed at different trench depths. Note that the RMS values are the subtraction of a bare wafer and a wafer processed with the oxide dot or the oxide dot and the trench etch.

Wafer	Trench Depth (µm)	RMS with oxide (nm)	RMS with oxide and trench (nm)	RMS reduction (%)
1	0	97.17	-	-
2	190	100.18	103.30	-1.03
3	260	104.47	61.65	40.98
4	300	89.24	42.35	52.54

Downloaded From: https://www.spiedigitallibrary.org/conference-proceedings-of-spie on 11 Sep 2019
Terms of Use: https://www.spiedigitallibrary.org/terms-of-use

4. CONCLUSION

In this paper, the concept of creating a trench around a stressed surface point, such as an oxide dot or epoxy dot was presented. This procedure has an application for reducing deformation caused by epoxy bond points for assembling X-ray optics in X-ray telescopes such as the Lynx X-ray telescope. Results showed that the P-V deformation of a 4 mm-diameter oxide dot on a 100 mm-diameter wafer with a thickness of 500 µm via simulated data was 888 nm, which was consistent with the 750 nm P-V deformation seen in the experimental data from the interferometer. Etch depths as deep as 300 µm were demonstrated via DRIE and showed that deeper trench etches allow for more deformation reduction. Based on all four etch depths, the data demonstrated reduction in deformation that starts when the etch was greater than 50% of the wafer thickness. We were also able to show verifications of this experimental data via simulations, which showed that there is promise for continuation of work in the area of this stress relief technique. Future work should expand the models to include more realistic X-ray mirrors such as Wolter-I mirrors in a meta-shell with multiple bond points[6]. In addition, now that we have metrology with a lower noise floor, work done with cured epoxy as opposed to thermal oxide should be explored and measured.

ACKNOWLEDGEMENTS

This work was supported by NASA Grant NNX16AD01G. Additional thanks to Will Zhang and others at NASA Goddard Space Flight Center (GSFC) for advice and Microsystems Technology Laboratory (MTL) at MIT for the use of the facilities fabrication tools.

REFERENCES

[1] Michael D. DeTienne, Alexander R. Bruccoleri, Anjelica Molnar-Fenton, Brandon Chalifoux, Ralf K. Heilmann, Youwei Yao, Mark L. Schattenburg, "X-ray telescope mirror mounting and deformation reduction using ThermoYield actuators and mirror geometry changes," Proc. SPIE 10699, Space Telescopes and Instrumentation 2018: Ultraviolet to Gamma Ray, 1069943 (6 July 2018);

[2] Koglin, J. E., An, H., Blaedel, K. L., Brejnholt, N.F., Christensen, F. E., Craig, W. W., Decker, T. A., Hailey, C. J., Hale, L. C., Harrison, F. A., Jensen, C. P., Madsen, K. K., Mori, K., Pivovaroff, M. J., Tajiri, G., Zhang, W. W., "NuSTAR hard x-ray optics design and performance," Proc. SPIE 7437, Optics for EUV, X-Ray, and Gamma-Ray Astronomy IV, 74370C (2009);

[3] Brejnholt, N. F., Christensen, F. E., Westergaard, N. J., Hailey, C. J., Koglin, J. E., Craig, W. W., "NuSTAR on-ground calibration: II. Effective area," Proc. SPIE 8443, Space Telescopes and Instrumentation 2012: Ultraviolet to Gamma Ray, 84431Y (2012);

[4] Westergaard, N. J., Madsen, K. K., Brejnholt, N. F., Koglin, J. E., Christensen, F. E., Pivovaroff, M. J., Vogel, J. K., "NuSTAR on-ground calibration: I. Imaging quality," Proc. SPIE 8443, Space Telescopes and Instrumentation 2012: Ultraviolet to Gamma Ray, 84431X (2012);

[5] Gaskin, J. A., Weisskopf, M. C., Vikhlinin, A., Tananbaum, H. D., Bandler, S. R., Bautz, M. W., Burrows, D. N., Falcone, A. D., Harrison, F. A., Heilmann, R. K., Heinz, S., Hopkins, R. C., Kilbourne, C. A., Kouveliotou, C., Kraft, R. P., Kravtsov, A. V., McEntaffer, R. L., Natarajan, P., O'Dell, S. L., Petre, R., Prieskorn, Z. R., Ptak, A. F., Ramsey, B. D., Reid, P. B., Schnell, A. R., Schwartz, D. A., Townsley, L. K., "The X-ray Surveyor Mission: a concept study," Proc. SPIE 9601, UV, X-Ray, and Gamma-Ray Space Instrumentation for Astronomy XIX, 96010J (2015);

[6] McClelland, R. S., Bonafede, J. A., Saha, T. T., Solly, P. M., Zhang, W. W., "Design and analysis of an x-ray mirror assembly using the meta-shell approach," Proc. SPIE 9905, Space Telescopes and Instrumentation 2016: Ultraviolet to Gamma Ray, 99057A (2016);

Downloaded From: https://www.spiedigitallibrary.org/conference-proceedings-of-spie on 11 Sep 2019
Terms of Use: https://www.spiedigitallibrary.org/terms-of-use